Optimal design of transverse ribs in tubes for thermal performance enhancement

Kyung Min Kim, Beom Seok Kim, Dong Hyun Lee, Hokyu Moon, Hyung Hee Cho*

Department of Mechanical Engineering, Yonsei University, 262 Seongsanno, Seodaemun-gu, Seoul 120-749, Republic of Korea

ABSTRACT

We conducted an optimization using the second-order response surface method to determine the transverse rib geometry required to achieve the highest cooling performance in a circular channel. The best rib geometry was based on three design variables; rib height, rib width, and rib pitch. The turbulent heat transfer coefficients and friction losses were first calculated and then used to determine the thermal performance. We constructed the response surfaces of the three design variables as functions of the average Nusselt number ratio, friction loss, and thermal performance. These functions led to the optimum design point at the highest heat transfer rate in the special case of an actual turbine cooling passage with a constant friction loss.

© 2010 Elsevier Ltd. All rights reserved.

1. Introduction

The improvement in energy efficiency in a gas turbine is closely related to the increase in turbine inlet temperature, which is accompanied by an excess thermal load on hot components of the turbine. Various cooling techniques have been used to protect the main hot areas in turbines, such as combustor liners, transition pieces, and turbine vanes/blades. In such a high-temperature environment, unsuitable cooling technology causes local thermal cracks and structural failures because of thermal stress and the reduction of material strength. Internal passage cooling is one cooling method used to protect gas turbine blades effectively because it covers most of the blade surfaces with minimal loss of the coolant fluid.

In recent turbine designs, internal passage cooling has been used in the third-row turbine blades as well as the first- and the second-row blades to help cope with the increasing turbine inlet temperature. Circular cooling passages with ribbed surfaces have been used because the second- and the third-row blades are longer and thicker than first-row blades. The passages in turbine blades are produced by shaped tube electrochemical machining drilling, which produces cooling channels with rib-roughened surfaces and results in a large enhancement of the heat transfer in the cooling

passage [1]. This enhancement occurs because the rib turbulators break the boundary layers, increase the turbulence intensity, induce reattachment flow between the ribs, and create a secondary or swirling flow structure. This technique is used in gas turbines [2] as well as in other energy industry fields such as solar air heaters [3] and evaporators/condensers [4].

Many studies [2–15] have noted that the internal cooling channel is characterized by many design parameters such as rib height (e), rib width (w), rib pitch (p), and rib attack angle (α), all of which greatly affect the enhancement of heat transfer and friction losses. Many researchers have addressed these geometries in rectangular channels [2,3,5–7] and circular channels [4,8–12], while others have investigated the effects of various rib turbulator shapes such as V-shaped ribs [13,14] and discrete ribs [15] on heat transfer in rectangular channels. More recently, combined methods of cooling and optimization [16–18] have been developed to provide effective internal cooling systems. The general response surface method (RSM) for optimizing the shape of the ribbed channels is suitable for choosing the best rib geometry for heat transfer enhancement. However, the general RSM based on the design variables has limitations due to narrow-design variable ranges and low physical responses. Due to these limitations, the optimum results are often different than previous experimental results.

Therefore, the objective of this study was to determine the rib height (h), rib width (w), and rib-to-rib pitch (p) that yield the maximum heat transfer and minimum friction loss using an

---

* Corresponding author. Tel.: +82 2 2123 2828; fax: +82 2 312 2159.
E-mail address: hhcho@yonsei.ac.kr (H.H. Cho).

Nomenclature

D	circular diameter (m)
D_h	hydraulic diameter (m), $D = D_h$
e	rib height (m)
f	friction factor
h	heat transfer coefficient (W m^{-2} K^{-1})
H	channel height (m)
l	rib-to-rib length (m)
k_c	conductivity of air
Nu	Nusselt number, hD_h/k_c
Nu$_{avg}$	average Nusselt number in one pitch
OF	objective function
p	rib-to-rib pitch, $l + w$
Pr	Prandtl number, $\mu C_p/k_c$

R^2	determined R squared
R^2_{adj}	adjusted determined R squared
Re	Reynolds number, $D_h u_b/v$
TP	thermal performance
u_b	passage inlet average bulk velocity (m s^{-1})
w	rib width (m)
W	channel width (m)

Greek symbols

β	polynomial coefficient
μ	dynamic viscosity (kg m^{-1} s^{-1})
ρ	air density
v	kinematic viscosity (m^2 s^{-1})
ΔP_p	pressure difference between inlet and outlet in one rib-to-rib pitch

advanced response method based on functional design variables with broader design variable ranges and higher physical responses than those in the general response method. We used a commercial software package (FLUENT 6.2) to analyze the heat transfer and friction loss. We obtained a variety of correlations with the functional design variables and determined the rib geometries with maximum heat transfer and thermal performance.

2. Research methods

2.1. Optimization technique (advanced response surface method)

Determination of the optimum dimensions related to many design parameters is often very important in engineering designs. The RSM is a well-known optimization technique that has the advantage of finding a correlation among the design variables, which can then be used to select design geometries with optimum values. Equations such as first- or second-order polynomials are generally used for the response surface based on approximations. Using these equations, we can search for the local optimum values within the region of interest using the method described by Myers and Montgomery [19]. However, the general RSM cannot be used with complex functions more than second-order, and has the drawbacks of low physical response (local sensitivity) and limited selection of design variable ranges because the formulas of the results are only parabolic in shape. Giunta [20] and Kim [21–23] proposed an advanced problem-solving method based on functional variables with thermal characteristics of the design variables. The advanced RSM procedure includes understanding the thermal characteristics of the design variables in a design range followed by changing the variables (x_i) into functional design variables ($f(x_i)$) as in this polynomial:

$$y = C_1 f(x_1)^2 + C_2 f(x_2)^2 + C_3 f(x_3)^2 + C_4 f(x_1)f(x_2) + C_5 f(x_2)f(x_3) \\ + C_6 f(x_3)f(x_1) + C_7 f(x_1) + C_8 f(x_2) + C_9 f(x_3) + C_{10} \quad (1)$$

subject to $f(x_i)$: $\sin(x_i)$, ..., $\log(x_i)$, ..., $\exp(x_i)$, etc., where $f(x_i)$ is determined through the process of understanding the thermal characteristics. These thermal characteristics are used to determine the trend of each variable from literature reviews and case-by-case studies. A fitting function is selected from among a variety of functions using the least mean square method. The functional RSM has certain advantages, such as the selection of wide ranges and close physical approximation. The results of the functional RSM are closer to the actual data than those of the non-functional RSM. Fig. 1 shows the overall procedure of the advanced RSM with functional variables The steps in the procedure are the following: select design variables and spaces in design parameters, understand the thermal characteristics

of the variables, construct design points using design of experiments (DOE), perform experiments or numerical analysis, perform regression analysis and analysis of variance (ANOVA), create the approximation equations, and determine the optimum values.

RSM was used in this study to obtain an optimal thermal design for an angled ribbed channel. In the RSM procedure, the unknown coefficients (C_i) of a second-order response surface polynomial (x_i) and function ($f(x_i)$) were determined using the least squares method. The set of design points was selected by the D-optimal method, which provides an efficient approach for response surface model building as suggested by Mitchell [24]. This is a useful and reliable method of constructing a response surface with a small number of design points, as few as only 1.5–2.5 times the number of unknown coefficients of the polynomial. When the observed
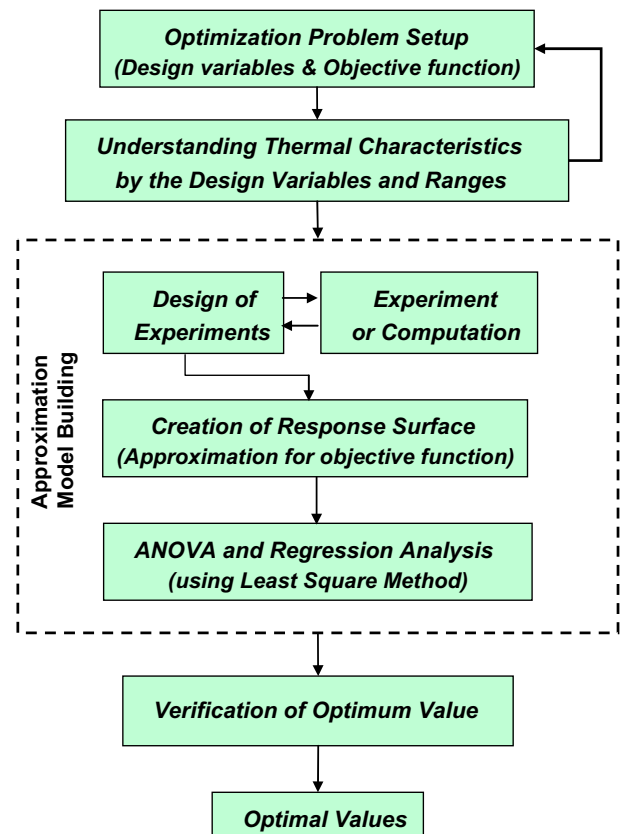

Fig. 1. Flowchart of the advanced RSM process.

response values are predicted accurately by the response surface model from the results of ANOVA, Guinta [20] suggested that the typical values of R^2_{adj} are in the range, 0.9–1.0. Also, the value of $1 - R^2_{adj}$ means a formulation error in each equation, and the maximum error in this study is approximately 5%.

2.2. Numerical analysis of fluid flow and heat transfer

The channel used for the thermal calculation had a circular cross-section with a diameter, $D = 3.81$ mm. The computation domain length was one pitch due to the periodic behavior of the flow in Fig. 2. All calculations in this study were conducted using FLUENT v 6.2. The Reynolds-averaged Navier-Stokes equations and the transport equations of the turbulent quantities were solved by the SIMPLE pressure-correction algorithm. The fluid was considered to be incompressible and the fluid properties were assumed to be constant. The SST $k−\omega$ model was selected as the turbulence model.

The grid for the computations consisted of 50,000–100,000 computational cells. Fig. 3(a) shows the computational grid details for the axisymmetric rib arrays. An exponential function was used to concentrate the fine mesh near the wall and rib surfaces to resolve the high-velocity gradients near the walls. The first grid point from the wall was carefully adjusted to be located in the linear region to ensure that y^+ was less than 1.0 [25]. In addition, we kept the maximum grid sizes constant when generating the grids.

Grid dependency tests were conducted using five different mesh sizes for the axisymmetric array of ribs at $e/D = 0.1$, $w/e = 1.0$, and $l/e = 9.0$, as shown in Fig. 3(b). A maximum grid size of 0.02 mm was selected as the optimum based on these results. The periodic conditions in all cases were set to a constant wall heat flux value of 50,000 W/m^2, a bulk velocity corresponding to a Reynolds number of 30,000, and a turbulence intensity of 5%.

2.3. Design variables and objective functions

A general ribbed channel with a circular cross-section has five parameters: channel diameter (D), rib height (e), rib width (w), rib-to-rib interval (l), and rib angle of attack (α). We selected three of these (rib height, rib width, and rib-to-rib interval) and converted them to dimensionless variables: rib height-to-channel diameter (e/D), rib width-to-rib height (w/e), and rib interval-to-rib height (l/e). Table 1 shows the ranges of these design variables.

To determine the maximum pitch-averaged heat transfer, maximum thermal performance, and minimum friction loss, the objective functions were defined as follows.

$$[F_{Nusselt}]_{max.} = \frac{Nu_{avg}}{Nu_0} \qquad (2)$$

where Nu_{avg} is the pitch-averaged Nusselt number and Nu_0 $(= 0.023Re^{0.8}Pr^{0.4})$ is the Nusselt number suggested by Dittus and Boelter [26] for fully developed turbulent flows in a smooth pipe.
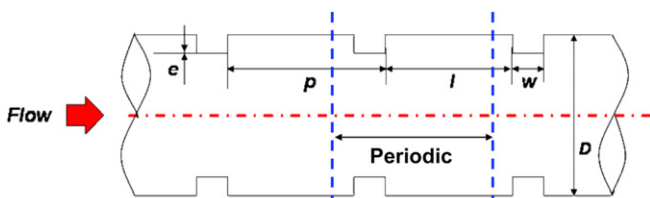

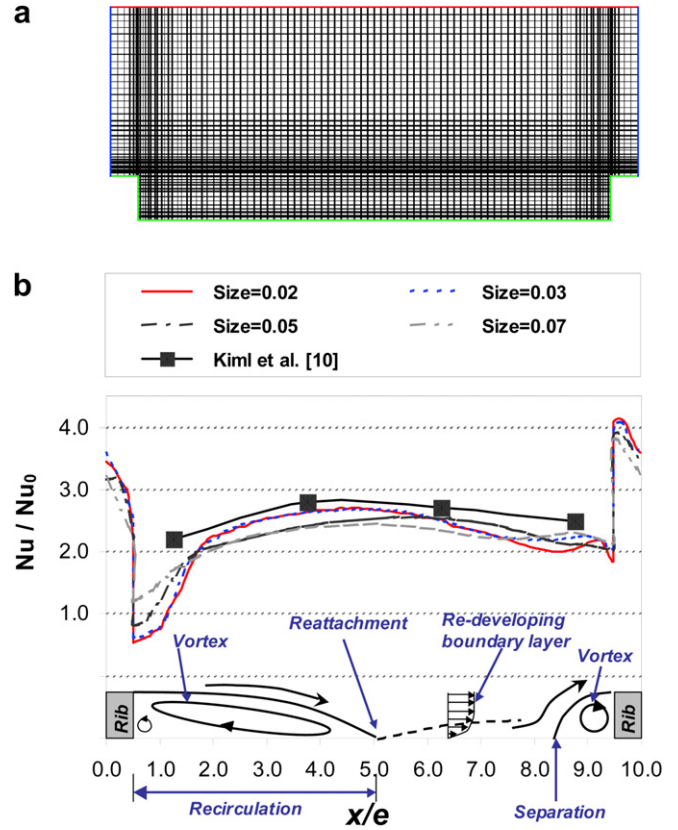**Fig. 2.** Geometric parameters and design variables.

Fig. 3. Grid tests at $e/D = 0.1$, $w/e = 1.0$, and $l/e = 9.0$: (a) grid details and (b) grid dependency.

$$\left[F_{friction}\right]_{min.} = \frac{f}{f_0} = \frac{(\Delta P_p/(4p/D))/\left(1/2 \cdot \rho \, u_b^2\right)}{2(2.236 \ln(Re) - 4.639)^{-2}} \qquad (3)$$

where the friction factor, f is calculated from the average pressure drop and f_0 represents the friction factor for a fully developed turbulent flow in a smooth pipe. An empirical equation that closely fits the Kármán-Nikuradse equation proposed by Petukhov [27] was used.

$$[F_{TP}]_{max.} = \frac{Nu_{avg}/Nu_0}{(f/f_0)^{1/3}} \qquad (4)$$

The objective function of the thermal performance (TP) was expressed by considering both the heat transfer augmentation and the friction loss under the condition of constant pumping power.

3. Results and discussion

3.1. Heat transfer and friction loss characteristics

Fig. 3 shows the grid details, grid independency test results, and a comparison with other studies of flow patterns in a ribbed channel. A grid size of 0.02 was selected as optimum based on the

Table 1
Design variables and ranges.

Design variable		Lower bound	Upper bound
x_1	e/D	0.01	0.15
x_2	w/e	0.25	5.0
x_3	l/e	2.0	12.0

grid independency test results. These were compared to the experimental results reported by Kiml et al. [10], who performed experiments with Re = 15,000, $e/D = 0.1$, $w/e = 1.0$, and $p/e = 10.0$. The experimental data had a distribution similar to the data in this study, but were of greater magnitude because the Reynolds number was higher. In general, normalized Nusselt numbers at low Re values are higher than those at high Re values, as noted by Webb et al. [8].

Transverse rib turbulators had the following three effects on flow structures and local heat transfer coefficients, as shown in Fig. 3(b). First, the main flow was separated by the rib turbulators. Second, the separated flow reattached in the inter-rib region 5−7 times the rib height downstream from the separation point, and thus the heat transfer in this region was enhanced. Third, the flow developed, the boundary layer thickened, and the heat transfer was reduced after the reattachment region. Because of these characteristics, the heat transfer and friction loss were influenced by the rib geometries such as rib height (e), rib width (w), and rib-to-rib pitch (p).

Fig. 4 shows the pitch-averaged Nu ratios and the friction losses to illustrate the thermal characteristics for each aspect of the rib geometry, $i.e.$, for each design variable. In addition, the calculated results were compared with the experimental correlations [9] used in actual heat exchanger design [12] and given below:

$$Nu/Nu_0|_{exp.} = \left\{ 1 + \left[2.64 Re^{0.036} \left(\frac{e}{D} \right)^{0.212} \right. \right.$$
$$\left. \left. \times \left(\frac{p}{D} \right)^{-0.21} Pr^{-0.024} \right]^7 \right\}^{1/7} \tag{5}$$

$$f/f_0|_{exp.} = \left\{ 1 + \left[71.9 Re^{(0.18-0.06p/D)} \left(\frac{e}{D} \right)^{(1.37-0.157p/D)} \right. \right.$$
$$\left. \left. \times \left(\frac{p}{D} \right)^{(-1.66E-6Re-0.33)} \right]^{15/16} \right\}^{16/15} \tag{6}$$

These correlations are widely used in the design of heat exchangers although effects of the rib width are not included.

Of all the design variables, the rib height was the main factor in heat transfer and friction loss. For example, as the rib height (e) increased, the Nu ratios and the friction losses also increased significantly, as shown in Fig. 4(a). This occurred because as the rib height increased, the main flow was accelerated by a reduction of the flow area, and the recirculation (counter) vortex was strengthened between the separation and reattachment points. The friction losses from the correlation line were similar to those in this study, but the Nu ratios did not match.

As the rib width (w) increased, the Nu ratios obtained from this study also increased until w/e was approximately 1.0, and then decreased afterwards while the friction losses decreased. However, both the Nu ratios and the friction losses from the correlation decreased within the present rib width range, as shown in Fig. 4(b). However, the numerical data indicated that the heat transfer and friction loss were higher than correlations due to additional reattachment of the separated flow on the upper surface of the rib turbulators for wider ribs. Furthermore, the correlations did not consider the effects of rib width, as shown in Eqs. (5) and (6).

Low heat transfer and friction loss appeared in cases with narrow rib-to-rib pitches (p); however, these values were high for rib-to-rib pitches greater than 4.0 because circulation flow between the inter-rib areas was generated in the narrow pitches, whereas flow reattachment was generated for inter-rib lengths greater than approximately 4.0. Note that there was peak point with high Nu

ratios and high friction losses at a certain inter-rib length. The correlation data [9] for short inter-rib lengths did not match the present data in this study. The correlations are thus difficult to use because they only consider the design of rib-roughened surfaces with long pitches.

As a result, high heat transfer and high friction loss can be obtained in designs with pitches of about 4.0 and high rib heights. Although the correlations [9] perform well for ribs with long pitches, we require new correlations for ribs with short pitches.

3.2. Optimal thermal design in design space

We performed an optimization to generate new correlations. In this optimization, the resultant functions were expressed as a second-order response surface with 10 unknown coefficients, as shown in Eq. (1). The thermal characteristics of the three design variables had parabolic and logarithmic distributions, as shown in Fig. 4 and summarized in Table 2. New design points must be
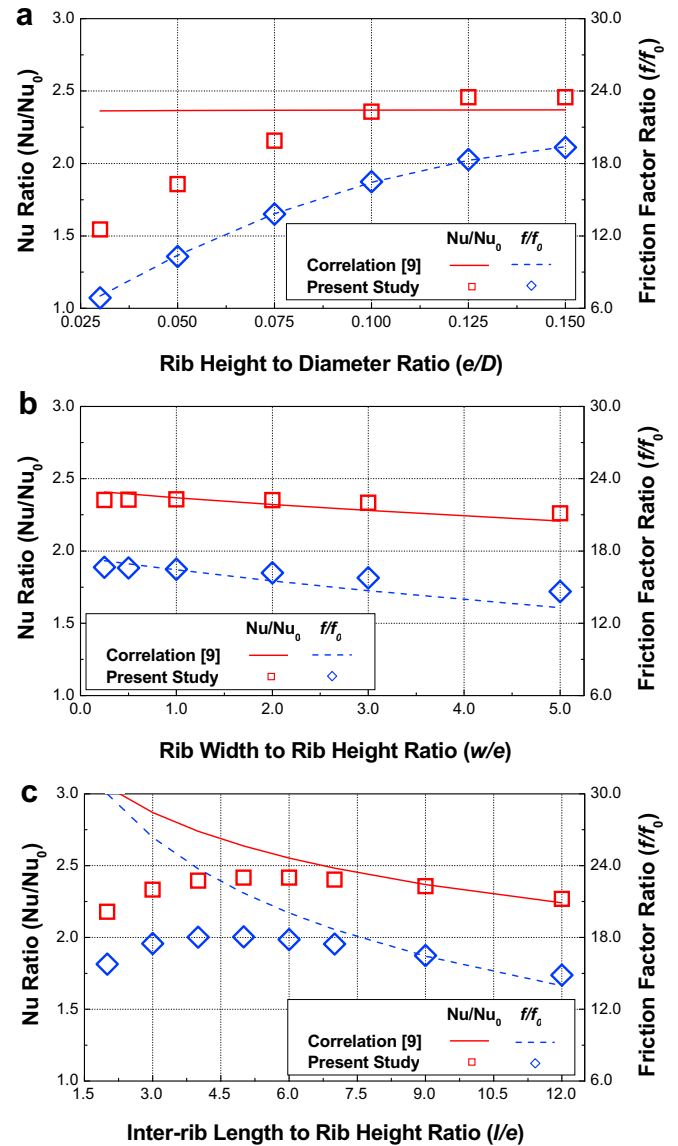

Fig. 4. Characteristics of each design variable and comparisons with experimental correlations [9]. (a) Effect of rib height at $l/e = 9.0$ and $w/e = 1.0$. (b) Effect of rib width at $e/D = 0.1$ and $l/e = 9.0$. (c) Effect of inter-rib distance at $e/D = 0.1$ and $w/e = 1.0$.

extracted within the design ranges to estimate the unknown polynomial coefficients. A total of 17 data points were selected by the D-optimal method [24], which is a DOE to spread out the design variables (data points). The previous 21 data points in 'Section 3.1' were added to these 17 data points. The polynomial coefficients (C_i) were estimated by the least squares method based on these analysis results for the 38 data points. The average Nu and friction ratios were then found using RSM according to:

- Average heat transfer ($R^2 = 0.981$, adj. $R^2 = 0.969$)

$$\begin{aligned} Nu_{avg}/Nu_0 = & -74.104(e/D)^2 - 0.0074(w/e)^2 - 1.261[\log(l/e)]^2 \\ & + 0.0298(e/D)(w/e) - 0.1603(w/e)\log(l/e) \\ & + 1.9235\log(l/e)(e/D) + 18.612(e/D) \\ & + 0.168(w/e) + 1.6503\log(l/e) + 0.6394 \end{aligned} \quad (7)$$

- Friction loss ($R^2 = 0.957$, adj. $R^2 = 0.951$)

$$\begin{aligned} f/f_0 = & -671.5(e/D)^2 - 0.0121(w/e)^2 - 18.202[\log(l/e)]^2 \\ & + 1.094(e/D)(w/e) - 0.766(w/e)\log(l/e) \\ & + 21.63\log(l/e)(e/D) + 203(e/D) + 0.065(w/e) \\ & + 22.248\log(l/e) - 3.22 \end{aligned} \quad (8)$$

In addition, the thermal performance (TP) in Eq. (4) was obtained from the Nu and friction factor ratios in both Eqs. (7) and (8).

Fig. 5 shows contour plots of the thermal performance obtained from Eqs. (7) and (8). The contour plots consist of TP maps in the design ranges of w/e and l/e for $e/D = 0.1$ (Fig. 5(a)), in the design ranges of l/e and e/D for $w/e = 1.0$ (Fig. 5(b)), and in the design ranges of w/e and e/D for $l/e = 9.0$ (Fig. 5(c)). The maximum thermal performance appeared for each case within the ranges of design variables: $l/e \geq 8.0$ and $2.0 \leq w/e \leq 3.0$ for $e/D = 0.1$, $0.10 \leq e/D \leq 0.12$ and $6.0 \leq l/e \leq 8.0$ for $w/e = 1.0$, and $0.10 \leq e/D \leq 0.12$ and $2.0 \leq w/e \leq 3.0$ for $l/e = 9.0$. The rib height (e/D) with the highest thermal performance can be expressed as:

- e/D with the highest TP at each w/e and l/e ($R^2 = 0.99$, adj. $R^2 = 0.989$)

$$\begin{aligned} [e/D]_{high,TP} = & 0.0000102(w/e)^2 - 0.000086[\log(l/e)]^2 \\ & - 0.00012(w/e)[\log(l/e)] - 0.00471(w/e) \\ & + 0.002412\log(l/e) + 0.1045 \end{aligned} \quad (9)$$

Thus, we have determined the optimal e/D in the design ranges of l/e and w/e.

The optimal rib heights can be drawn in the design space, as shown in Fig. 6. The optimal design surface with the highest thermal performance existed in the design range of e/D from 0.100 to 0.125. The height of high-performance ribs increased as the rib width increased or as the inter-rib decreased. Fig. 7(a) shows the Nu

Table 2
Summary of thermal characteristics by each variable.

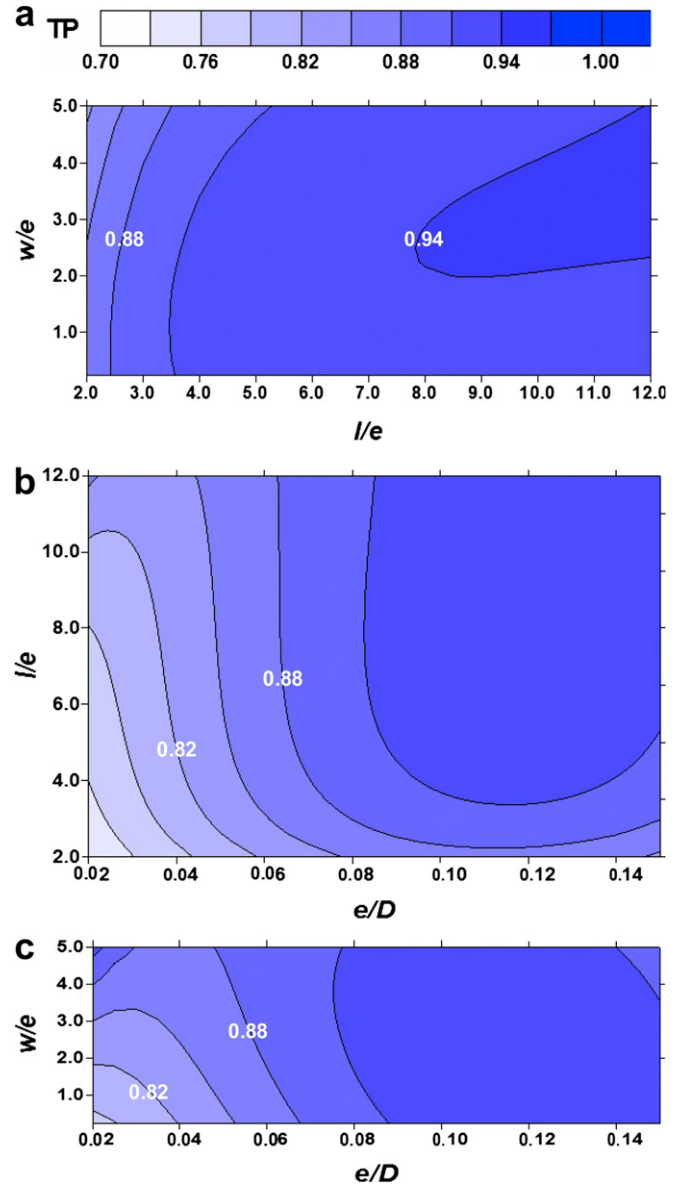| Variables		Results	
		Nu/Nu_0	f/f_0
x_1	e/D	$C_1 x_1^2 + C_2 x_1 + C_3$	
x_2	w/e	$C_1 x_2^2 + C_2 x_2 + C_3$	
x_3	l/e	$C_1[\log(x_3)]^2 + C_2\log(x_3) + C_3$	

Fig. 5. Thermal performance for various design variables. (a) TP for $e/D = 0.1$. (b) TP for $w/e = 1.0$. (c) TP for $l/e = 9.0$.

ratios, Fig. 7(b) shows the friction losses, and Fig. 7(c) shows the thermal performance for the optimal rib heights shown in Fig. 6. In an actual design, we recommend ranges of $5.0 \leq l/e \leq 6.5$ and $0.25 \leq w/e \leq 1.0$ for high heat transfer, and ranges of $8.0 \leq l/e \leq 10.0$
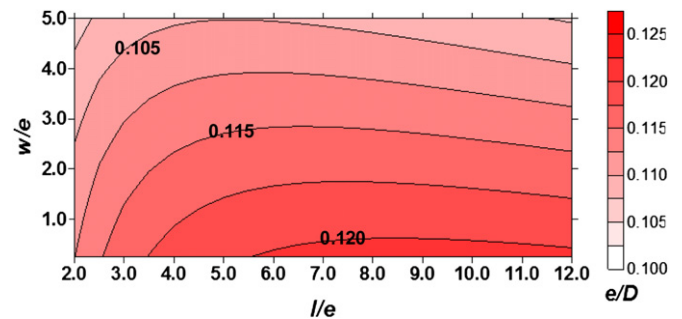
Fig. 6. Optimal results of e/D with the highest TP for each l/e and w/e in the design space.
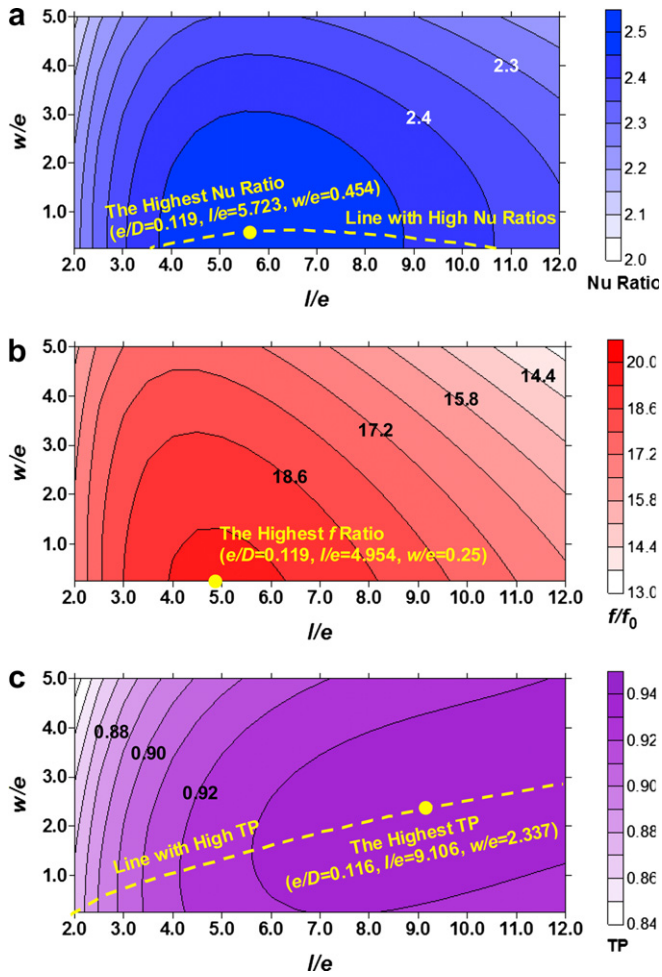
Fig. 7. Thermal results on the design surface with the highest TP for each l/e and w/e. (a) Nu ratio. (b) Friction factor ratio. (c) Thermal performance.
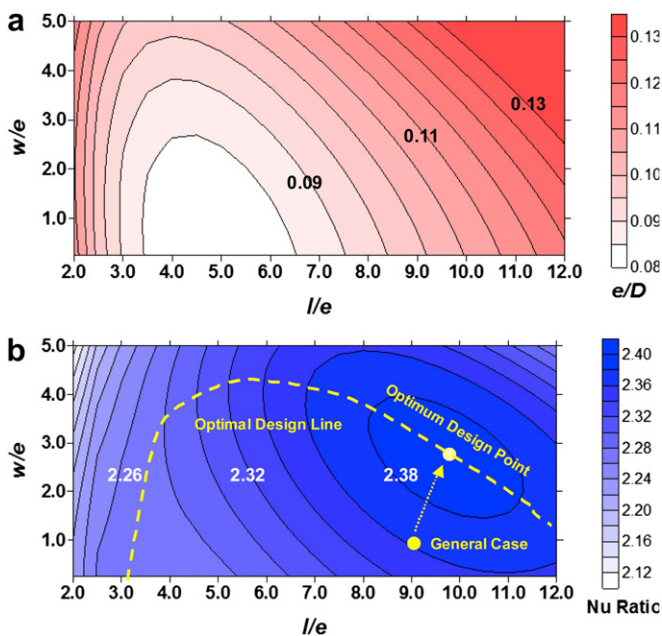

Fig. 8. Maps for the specific case of f/f_0 of 13.482. (a) Ratios of rib height-to-channel diameter. (b) Optimal map of Nu ratios.

and $1.5 \leq w/e \leq 2.5$ for high-performance. However, we do not recommend design ranges of $4.5 \leq l/e \leq 5.5$ and $0.25 \leq w/e \leq 0.5$ because of the high friction loss. The greatest heat transfer appeared at $e/D = 0.119$, $l/e = 5.723$, and $w/e = 0.454$; the highest friction loss appeared at $e/D = 0.119$, $l/e = 4.954$, and $w/e = 0.25$; and the highest thermal performance appears at $e/D = 0.116$, $l/e = 9.106$, and $w/e = 2.337$.

3.3. Optimal thermal design for a special case

We sometimes need to design rib geometries for a fixed flow rate with a certain friction factor ratio to enhance the energy efficiency from a compressor while maintaining the same pumping power. As an example, a study was performed to obtain a high heat transfer rate with the same friction loss in general rib geometries. Fig. 8 shows the contour maps of rib height-to-channel diameter ratios and Fig. 8(b) shows the pitch-averaged Nu ratios for various values of w/e and l/e in the special case of a friction factor ratio of 13.482 for $e/D = 0.1$, $l/e = 9.0$, and $w/e = 1.0$. These design conditions were used for an actual turbine blade. The rib height ratio (e/D) at constant friction loss was obtaining by setting $f/f_0 = 13.482$ in Eq. (8) within ranges of two variables. The following equation for e/D as a function of w/e and l/e was produced using the least mean square method:

- e/D at $f/f_0 = 13.482$ ($R^2 = 1.0$, adj. $R^2 = 1.0$)

$$[e/D]_{\text{Const.}f} = 0.0007572(w/e)^2 + 0.234749[\log(l/e)]^2$$
$$+ 0.007377(w/e)[\log(l/e)] - 0.005154(w/e)$$
$$- 0.317952\log(l/e) + 0.18794 \qquad (10)$$

We can now determine the new design point with the highest heat transfer rate for a given friction loss based on the contour plot of the response surface shown in Fig. 8(b). The optimum design point with the highest Nu ratio appeared at $l/e = 9.694$ and $w/e = 2.753$. Using this optimization method, the heat transfer rate of the general cooling system could be enhanced 1.3% from 2.36 to 2.39. Furthermore, the optimum design line (the dashed line in Fig. 8(b)) for high heat transfer was obtained for a given l/e (distance between inter-ribs) as follows:

Optimal design line ($R^2 = 0.998$, adj. $R^2 = 0.994$)

$$[w/e]_{\text{Const.}f} = 40.371[\log l/e]^3 - 123.82[\log l/e]^2 + 117.32(l/e)$$
$$- 31.275 \qquad (11)$$

Even though this example based on the general geometries of an actual gas turbine blade yielded only a very small improvement in the heat transfer rate because of special boundary conditions, this method will provide significant energy efficiency improvements when determining the optimal configuration of rib turbulators for a limited flow rate in the initial design stage of a gas turbine.

4. Conclusions

The rib height (e), rib width (w), and inter-rib spacing (l) of transverse rib turbulators in a circular channel were investigated to enhance the heat transfer and the thermal performance using the RSM based on an approximation with functional variables. The conclusions can be summarized as follows.

1. The rib height (e) was the dominant factor in heat transfer and friction loss. As the rib height (e) increased, the Nu ratios and friction losses increased significantly because of the flow

acceleration and the large flow recirculation. As the rib width (w) increased, the Nu ratios and friction losses decreased because the flow reattachment location moved closer to the rib turbulators.

2. In a design space consisting of three design variables, the optimal e/D (rib height) with the highest thermal performance was in the design range from 0.100 to 0.125 for various values of w/e and l/e.

3. As a result of the optimization for the special case of $f/f_0 = 13.482$ representing an actual turbine cooling passage, the optimum design point was at $w/e = 2.753$ and $l/e = 9.694$, resulting in an average heat transfer improvement of 1.3% over the general case ($e/D = 0.1$, $l/e = 9.0$ and $w/e = 1.0$). This method can be used to obtain the optimal condition for a constant pumping power when designing actual turbine blades.

Acknowledgments

References

[1] Beddard TB, Collado CA. Airfoil cooling holes. United States Patent. US 2005/0129515 A1; 2005.
[2] Han JC, Park JS, Lei CK. Heat transfer enhancement in channels with turbulence promoters. J Eng Turbines Power 1985;107:628–35.
[3] Karwa R, Solanki SC, Saini JS. Thermo-hydraulic performance of solar air heaters having integral chamfered rib roughness on absorber plates. Energy 2001;26(2):161–76.
[4] Ravigururajan TS, Bergles AE. Optimization of in-tube enhancement for large evaporators and condensers. Energy 1996;21(5):421–32.
[5] Habib MA, Mobarak AM, Attya AM, Aly AZ. An experimental investigation of heat-transfer and flow in channels with streamwise-periodic flow. Energy 1992;7(11):1049–58.
[6] Maeda N, Hirota M, Fujita H. Turbulent flow in a rectangular duct with a smooth-to-rough step change in surface roughness. Energy 2005;30(2–4):129–48.
[7] Rau G, Cakan M, Moeller D, Arts T. The effect of periodic ribs on the local aerodynamic and heat transfer performance of a straight cooling channel. ASME J Turbomachinery 1998;120:368–75.
[8] Webb RL, Eckert ERG, Goldstein RJ. Heat transfer and friction in tubes with repeated-rib toughness. Int J Heat Mass Transfer 1971;14:601–17.
[9] Ravigururajan TS, Bergles AE. Development and verification of general correlations for pressure drop and heat transfer in single-phase turbulent flow in enhanced tubes. Exp Therm Fluid Sci 1996;13:55–70.
[10] Kiml R, Magda A, Mochizuki S, Murata A. Rib-induced secondary flow effects on local circumferential heat transfer distribution inside a circular rib-roughened tube. Int J Heat Mass Transfer 2004;47:1403–12.
[11] San J-Y, Huang W-C. Heat transfer enhancement of transverse ribs in circular tubes with consideration of entrance effect. Int J Heat Mass Transfer 2006;47:2965–71.
[12] Thome JR. Engineering data book III. Wolverine Tube Inc.; 2008.
[13] Lau SC, Kukreja RT, McMillin RD. Effects of V-shaped rib array on turbulent heat transfer and friction of fully developed flow in a square channel. Int J Heat Mass Transfer 1991;34(7):1605–16.
[14] Lee DH, Rhee D-H, Kim KM, Cho HH, Moon H-K. Detailed measurement of heat/mass transfer with continuous and multiple V-shaped ribs in rectangular channel. Energy 2009;34:1770–8.
[15] Cho HH, Wu SJ, Kwon HJ. Local heat/mass transfer measurements in a rectangular duct with discrete ribs. ASME J Turbomachinery 2000;122:579–86.
[16] Kim H-M, Kim K-Y. Design optimization of rib-roughened channel to enhance turbulent heat transfer. Int J Heat Mass Transfer 2004;47:5159–68.
[17] Kim H-M, Kim K-Y. Shape optimization of three-dimensional channel roughened by angled ribs with RANS analysis of turbulent heat transfer. Int J Heat Mass Transfer 2006;49:4013–22.
[18] Lee H, Kim KM, Lee DH, Cho HH. Optimization of angled ribs for heat transfer enhancement in a square channel with bleed flow. Trans KSME(B) 2008;32 (4):300–6.
[19] Myers RH, Montgomery DC. Response surface methodology: progress and product optimization using designed experiments. New York: John Wiley and Sons; 2002.
[20] Guinta AA. Aircraft multidisciplinary design optimization using design of experimental theory and response surface modeling methods. Ph.D. thesis, Virginia Polytechnic Institute and State University; 1997.
[21] Kim KM, Lee DH, Cho HH, Kim MY. Heat transfer in a ribbed circular passage of a gas turbine blade. In: Proceeding of 2008 KSME Spring Annual Meeting, Korea; 2008. p. 203–6.
[22] Kim KM, Kim BS, Lee DH, Moon H, Cho HH. Optimal cooling design of transverse rib turbulators in a circular channel. In: Proceedings of the Asian Congress on Gas Turbines. Paper No. ACGT2009–TS34; 2009.
[23] Kim KM, Lee H, Kim BS, Shin S, Lee DH, Cho HH. Optimal design of angled rib turbulators in a cooling channel. Heat Mass Transfer 2009;45(12):1617–25.
[24] Mitchell TJ. An algorithm for the construction of D-optimal designs. Technometrics 1974;20:203–10.
[25] Fluent 6.2 user's guide. Fluent Inc.; 2003.
[26] Dittus FW, Boelter LMK. Heat transfer in automobile radiations of tubular type. Int Commun Heat Mass Transfer 1985;12:3–22.
[27] Prabhu SV. Advances in heat transfer 6. New York: Academic Press; 1970. p. 503–64.